International Journal of Physics, 2017, Vol. 5, No. 4, 110-115
Available online at http://pubs.sciepub.com/ijp/5/4/2

DOI:10.12691/ijp-5-4-2

Annealing Effect on $(SnO_2)_{0.3}$:$(In_2O_3)_{0.7}$ Solar Cell Prepared by PLD Technique

Abdulmajeed E. Ibrahim[1], Kadhem A. Aadim[2], Qutaibah A. Abduljabbar[1,*]

[1]Department of Physics, University of Tikrit/College of Education
[2]Department of Physics, University of Baghdad / College of Sciences
*Corresponding author: qutaibahalrawi5378@gmail.com

Abstract Indium tin oxide (ITO) thin films were produced by Q- switched Nd:YAG laser with wavelength (1064 nm) has 800 mJ peak energy on In_2O_3 :SnO_2 target with 0.3 ratio on p-type Si and on porous Si to fabricated solar cell. The as deposited and annealed thin films on glass substrates were characterized by X-ray diffraction Atomic force microscopy (AFM), UV-visible absorbance and Hall effect measurements. Then the fabricated solar cells examined in the dark and under illumination for SnO_2:In_2O_3 /p-Si and SnO_2:In_2O_3/Psi/p-Si annealed and as deposited samples.

Keywords: *solar cell, pulse laser, porous-Si*

Cite This Article: Abdulmajeed E. Ibrahim, Kadhem A. Aadim, and Qutaibah A. Abduljabbar, "Annealing Effect on $(SnO_2)_{0.3}$:$(In_2O_3)_{0.7}$ Solar Cell Prepared by PLD Technique." *International Journal of Physics*, vol. 5, no. 4 (2017): 110-115. doi: 10.12691/ijp-5-4-2.

1. Introduction

Now a day there are many techniques utilized to enhance solar cell efficiency enhance solar cells efficiency [1].

The generic solar cell is a structure consisting of two active layers, thin heavily doped top layer called the emitter or window layer and thick moderately doped bottom layer, called the base or absorber with opposite doping [2]. We need to study the optical, structural [3], morphological [4] and electrical properties for used material as window in solar cells on the side where light enters, to reach optimum efficiency [5]

X- ray diffraction used to characterize obtained films crystallinety. The d_{hkl} spacing between crystals planes can deduced by X-ray diffraction using Bragg's law [6]

$$n\lambda = 2d_{hkl}\sin\Theta \quad (1)$$

where Θ is diffraction angle and λ is the used XRD wavelength.

Scherrer equation formula used to calculate crystalline size utilize the peaks broadening [7].

$$G.S = \frac{0.9\lambda}{FWHM\ .\ \cos(\theta)} \quad (2)$$

Where λ is the x-ray wavelength for k_α transition from Cu target (1.5406 Å), FWHM is full width at half maximum and θ is the angle of diffraction.

Several parameters are used to characterize solar cells. A solar cell under illumination is characterized by the following parameters: the Short-circuit current, the open-circuit voltage, the fill factor and the power conversion efficiency [8]. Fill Factor indicates the quality of current-voltage characteristics and it depends on the ability of charges to reach the electrodes which is governed by recombination processes. The full factor is directly affected by the values of the cell's series and shunt resistances [9]. The solar cell efficiency is the ratio for outcome power to incident light power density [10].

2. Experimental Part

A porous silicon structure is prepared by electrochemical etching of silicon substrate of (111) orientation with a resistivity (4 -10) Ω. cm and the etching cell is made of Teflon. The electrochemical cell used has two electrode configurations with a platinum electrode as cathode and silicon wafer as anode. The etching times is chosen to be 10 min and current (30) mA. The samples are dipped in (48%) concentration of (HF) acid in mixing ratio (1 : 1) HF: ethanol with the aid of diode laser source as an illumination sources. However, the addition of ethanol to HF eliminates hydrogen and ensures complete infiltration of HF solution which further improves the uniform distribution of porosity and thickness.

In_2O_3 with purity (99.9 %) and SnO_2 powder purity (99.98 %) by FERAK company, England were mixed with In_2O_3:SnO_2 ratio 30 % in gate mortar to use it to make pellet target as a disk of 1.5cm diameter using hydraulic piston under pressure of 6 tons.

SnO_2: In_2O_3 thin films were prepared on glass, p-Si and porous-Si substrates by Q switched pulsed laser (Huafei Tongda Technology- DIAMOND-288 pattern EPLS) λ = 1064 nm with 800 mJ peak power inside a vacuum chamber at vacuum (10^{-3} Torr) using double stage rotary pump. The incident beam coming through a window making an angle of 45° with the target surface. The substrate is placed

parallel target surface. The produced films were characterized by X-ray diffraction (XRD), DC conductivity, Hall effect measurements and UV-visible absorption

Metal electrodes of aluminum are formed both back surface of the Si wafer and top of the SnO_2:In_2O_3 films by thermal evaporation, carried out at a pressure of (10^{-5} mbar) in a vacuum (Edwards Auto 306). Annealing at 773K for 2 hours to enhance the films properties and its adhesion.

I-V measurements were made for fabricated solar cell heterojunctions in case of dark and under illumination by Halogen lamp light Philips (120W) with 100 mW/cm^2 intensity using Keithley Digital Electrometer 616, voltmeter and D.C. power supply under reverse and forward bias voltage in the range (-2 to 2) Volt to study the effect of annealing and porous formation on solar cells efficiency.

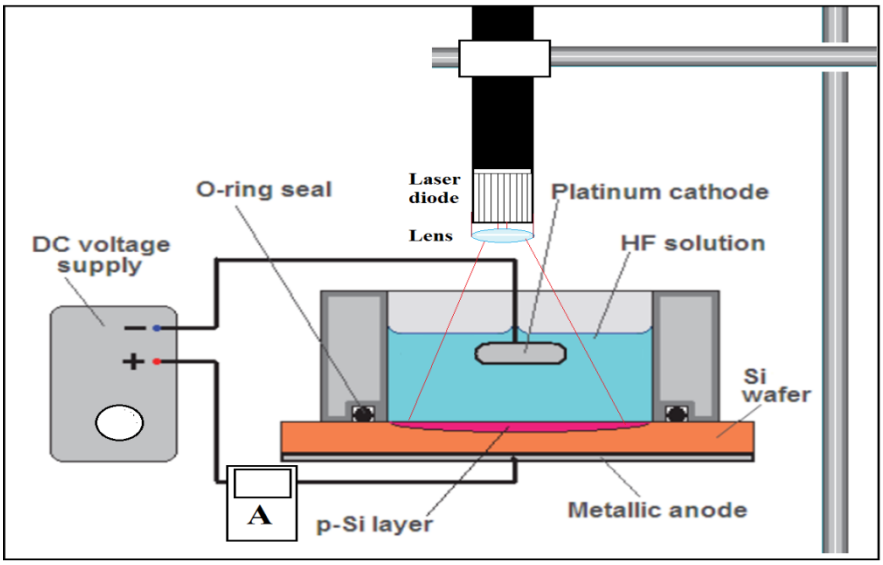

Figure 1. Schematic for porous silicon layer formation system

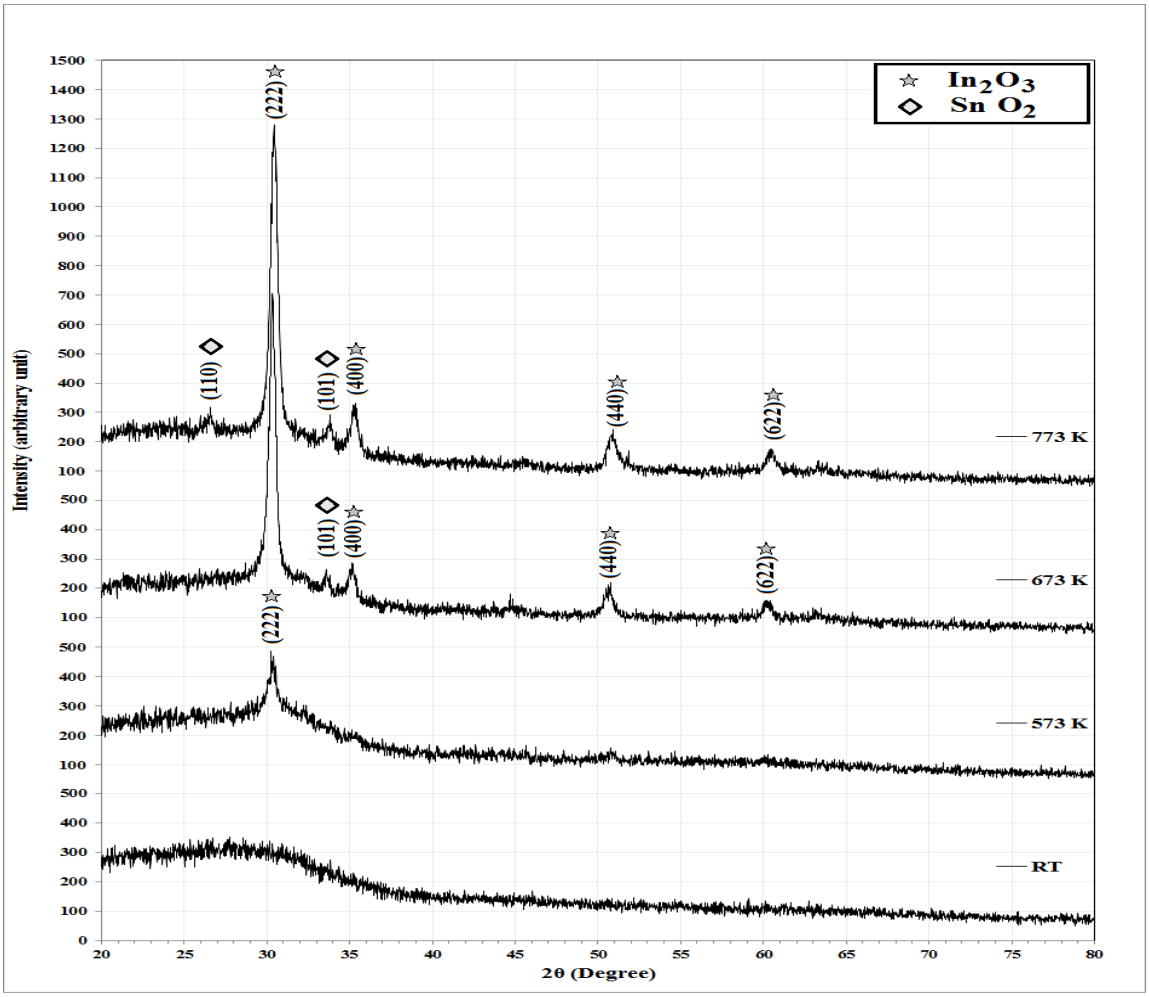

Figure 2. XRD patterns for In_2O_3:SnO_2 thin films annealed at different temperature

3. Results and Discussion

Figure 2 shows the X-ray diffraction for as deposited In_2O_3:SnO_2 with 0.3 ratio films deposited on glass substrates by pulse laser deposition and annealed at different temperatures (573, 673and 773) K. We can observe from this figure that as deposited film has amorphous structure at RT, while annealed one at 573 K, convert to polycrystalline structure, and with annealing at 673 K many peaks corresponding to In_2O_3 and one peaks for SnO_2. The crystallinety increase with increasing annealing to 773 K and their location shift toward higher values indicate on increase atomic backing with annealing. The FWHM decrease with increasing annealing temperature indicate on increasing G.S. Table 1 shows the experiment and the standard peaks from international center for diffraction data JCPD cards number (96-210-4744 and 96-101-0589).

Figure 3 shows the AFM images and their granularity accumulation distribution for as deposited In_2O_3 :SnO_2 with 0.3 ratio films deposited on glass substrates by pulse laser deposition and annealed at different temperatures (573, 673and 773) K. This figure and Table 2 illustrate that the average diameter and RMS roughness decrease with increasing annealing temperature.

Table 1. Comparison between experimental and standard XRD peak and calculated crystalline size

T (K)	2θ (Deg.)	FWHM (Deg.)	d_{hkl} Exp.(Å)	G.S (nm)	hkl	d_{hkl} Std.(Å)	Phase	Card No.
RT	Amorphous							
573	30.2314	0.8770	2.9540	9.4	(222)	2.9214	In_2O_3	96-101-0589
	30.3776	0.5115	2.9401	16.1	(222)	2.9214	In_2O_3	96-101-0589
	33.5932	0.2923	2.6656	28.4	(101)	2.6439	SnO_2	96-210-4744
673	35.1279	0.5846	2.5526	14.3	(400)	2.5300	In_2O_3	96-101-0589
	50.6943	0.8039	1.7993	10.9	(440)	1.7890	In_2O_3	96-101-0589
	60.1218	0.7308	1.5378	12.6	(622)	1.5256	In_2O_3	96-101-0589
	26.5043	0.5116	3.3603	16.0	(110)	3.3498	SnO_2	96-210-4744
	30.3776	0.4385	2.9401	18.8	(222)	2.9214	In_2O_3	96-101-0589
773	33.7393	0.4385	2.6544	18.9	(101)	2.6439	SnO_2	96-210-4744
	35.3471	0.4385	2.5373	19.0	(400)	2.5300	In_2O_3	96-101-0589
	50.8404	0.8039	1.7945	10.9	(440)	1.7890	In_2O_3	96-101-0589
	60.4872	0.6577	1.5294	14.0	(622)	1.5256	In_2O_3	96-101-0589

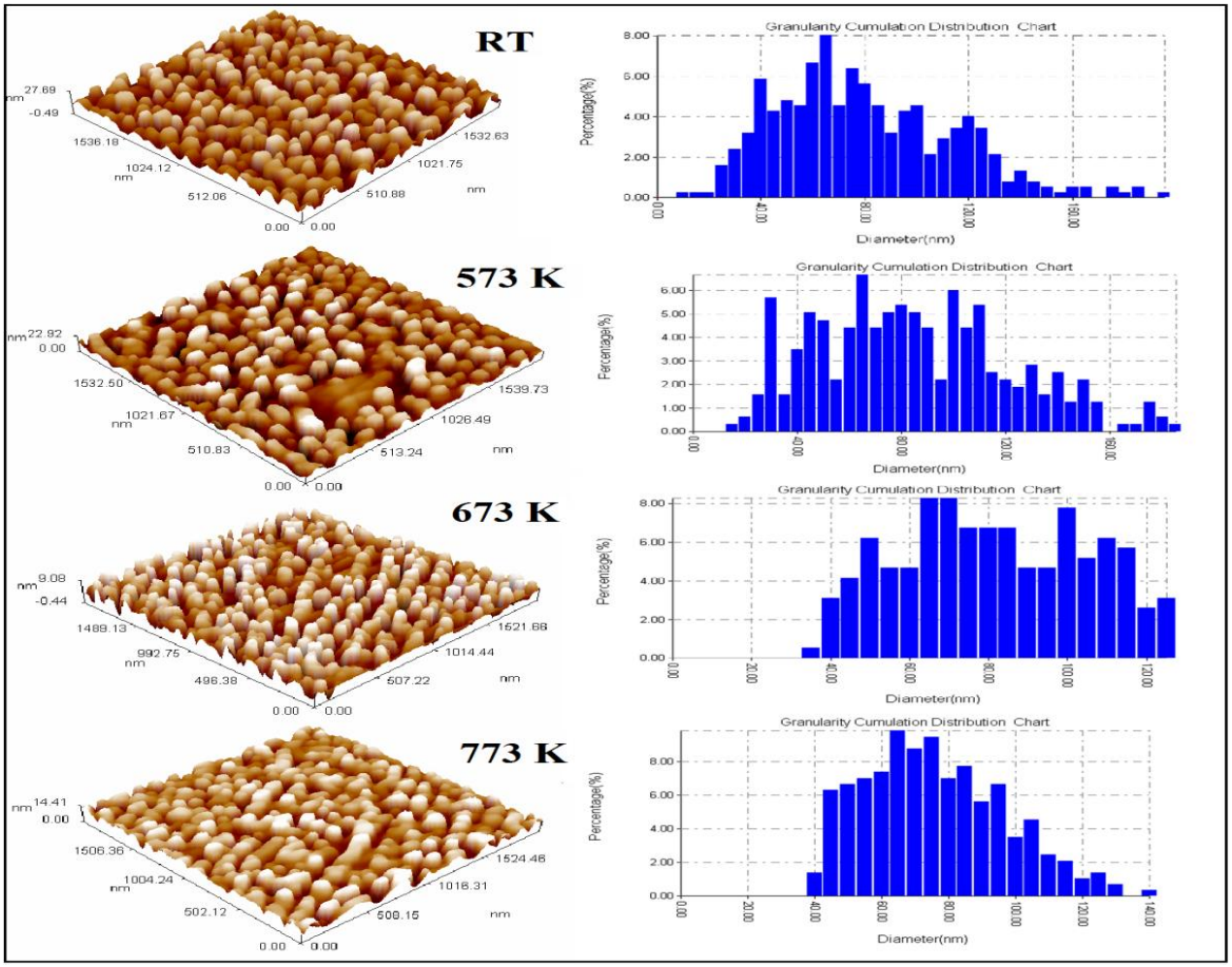

Figure 3. AFM images and their granularity accumulation distribution for In_2O_3 :SnO_2 =0.3 thin films deposited on glass substrate annealed at different temperature

Table 2. AFM parameters (Average Diameter, RMS roughness and Peak-peak distance) for pure for In_2O_3 :SnO_2 =0.3 thin films at different annealing temperature

T_a (K)	Average Diameter (nm)	RMS roughness (nm)	Peak-peak (nm)
RT	82.23	6.12	24.4
573	78.67	5.54	22.9
673	77.54	2.55	9.52
773	73.51	2.81	14.4

Figure 4 shows the transmission spectra for In_2O_3:SnO_2 annealed at different temperature. It shows that the transmission increase with increasing annealing temperature reaching 85% in visible range, as a result of enhance the crystallinety [11].

The optical energy gap values (E_g^{opt}) for In_2O_3:SnO_2 composite films at different annealing temperature have been determined by using Tauc equation as shown in Figure 5. From this figure seems that the energy gap increase from (2.8 to 3.7) eV with increasing annealing temperature as a result of increasing atomic backing with annealing [12].

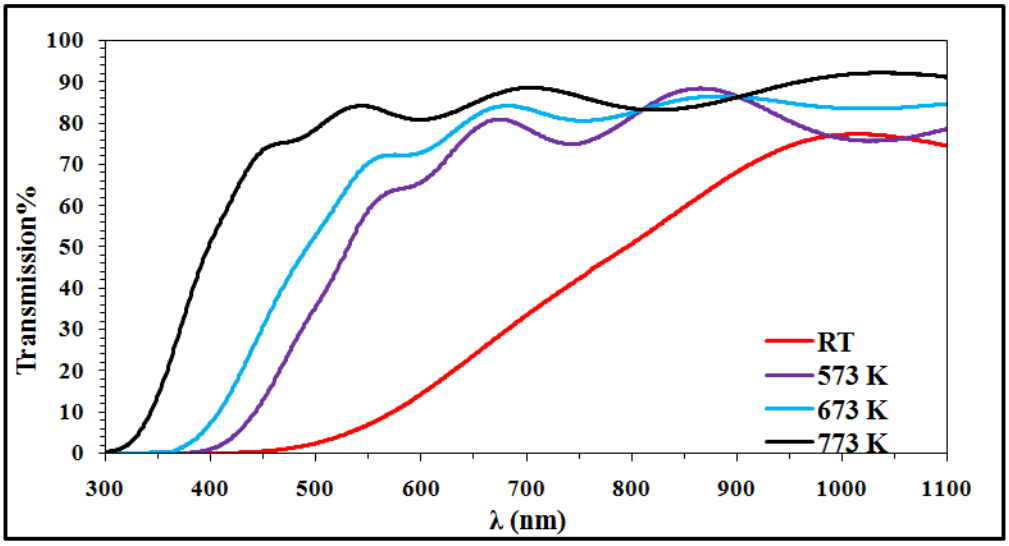

Figure 4. The variation of transmission with wavelength for In_2O_3 :SnO_2 =0.3 thin films deposited on glass substrate annealed at different temperature

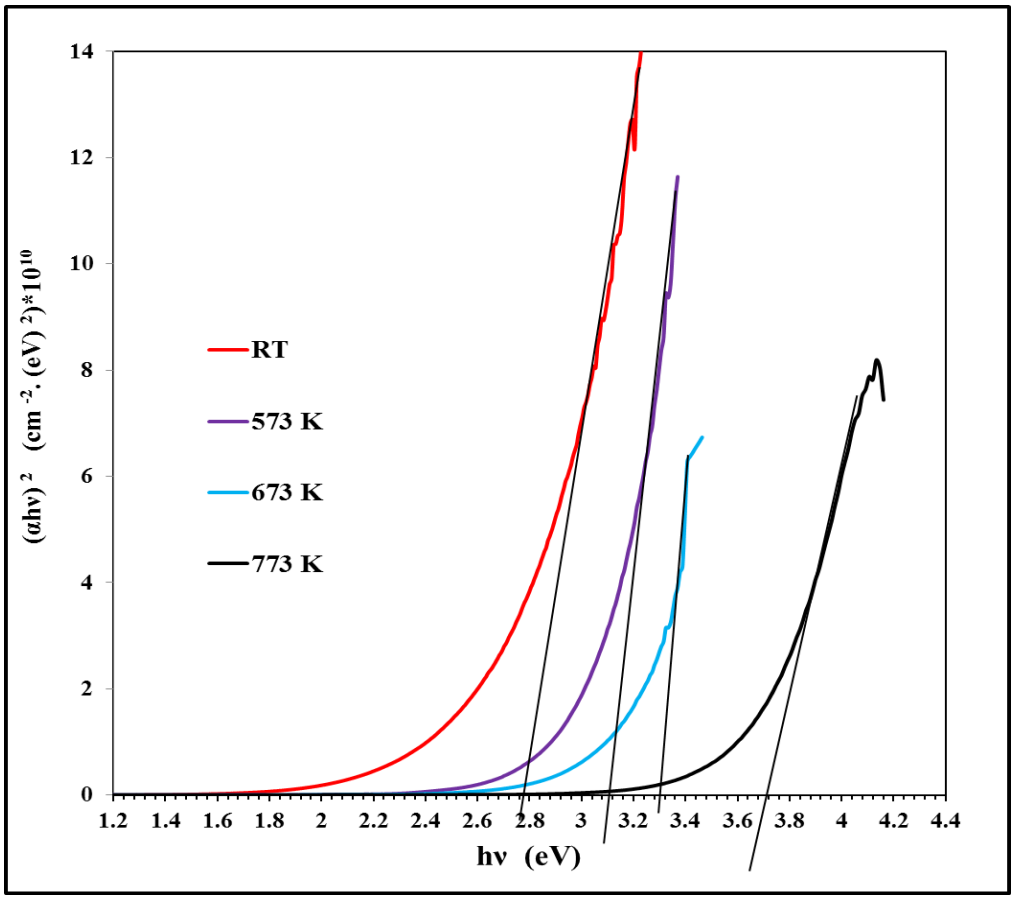

Figure 5. Variation of $(\alpha h\upsilon)^2$ versus photon energy for In_2O_3 :SnO_2 thin films with different annealing

Hall effect measurements show that all films were (n-type). The variation of n_H and μ_H with annealing temperature were shown in Table 3. The values of (n) increases with increasing annealing temperature reaching the maximum value at 673 K then decrease with more annealing. While the maximum value of electron mobility at 573 annealing temperature.

The I-V characteristics of SnO_2:In_2O_3/p-Si and SnO_2:In_2O_3/porous-Si solar cell with 0.3 In_2O_3 content, in the dark and under illumination using power densities equal to 100 mW/cm^2 with the applied forward and reverse bias voltage for RT and annealed at (773)K were shown in Figure 6. The solar cells parameters were shown in Table 4. This table shows that in general the annealed ones best than as deposited films and the samples deposited on porous Si best than that deposited on Si wafers.

From the plot of the forward current (I_f) versus applied forward bias voltage (V_f), the ideality factor (β) is obtained according to the relation [13]

$$\beta = \frac{q}{k_B T} \frac{dV_f}{d[\ln(I_f / I_s)]} \quad (3)$$

where I_s is the saturation current and it can be obtained by extrapolating the forward current curves to zero voltage.

Table 3. Hall measurements of for In_2O_3:SnO_2 composite thin films with different annealing temperature

T_a(K)	σ_{RT} (Ω^{-1}.cm^{-1})	R_H	n (cm^{-3})	type	μ_H (cm^2/v.sec)
RT	9.4×10^{-5}	110000	5.68×10^{13}	n	10.40
573	18.00	2.51	2.49×10^{18}	n	45.18
673	21.0	0.22200	2.82×10^{19}	n	4.66
773	15.00	0.07750	8.06×10^{19}	n	1.16

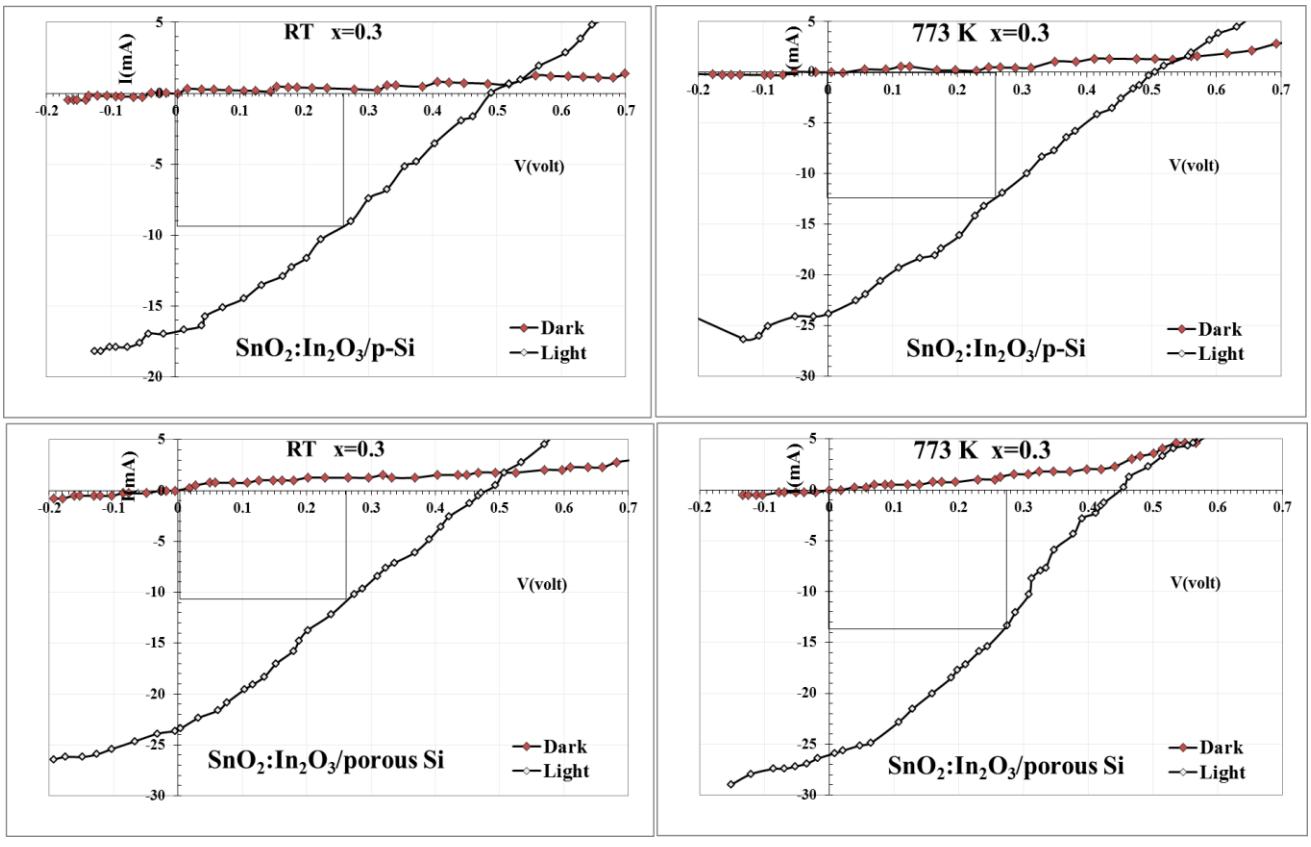

Figure 6. I-V characteristics for SnO_2 :In_2O_3/P-Si and SnO_2 :In_2O_3/porous-Si heterojunction Solar Cell at RT and 773 K annealing temperatures in case of dark and under illumination

Table 4. I-V Parameters for SnO_2 :In_2O_3/p-Si and SnO_2 :In_2O_3/porous-Si solar cell

Substrate	Ta (K)	I_{sc} (mA)	V_{oc} (V)	I_m (mA)	V_m(v)	F.F	η%	β
P-type Si	RT	17.00	0.49	9.50	0.26	0.30	2.47	3.810
	773	24.00	0.50	12.50	0.26	0.27	3.25	2.110
Porous Si	RT	23.50	0.48	11.00	0.26	0.25	2.86	3.636
	500	26.00	0.45	14.00	0.28	0.34	3.92	3.636

4. Conclusions

The results of examination of In_2O_3 :SnO_2 thin films deposited on glass substrates by XRD by pulse laser deposition show that annealing convert amorphous structure to polycrystalline structure with peaks corresponding to In_2O_3 and SnO_2. The crystallinety and the crystalline size increase with increasing annealing to 773 K.

The UV visible easements shows that the annealing leads to increase transparency and increase energy gap from 2.8 to 3.7 eV.

Hall effect measurements shows n-type for all films. The charge carrier concentration has maximum value at 673 K, while the maximum value of electron mobility at 573 annealing temperature.

The results for fabricated solar cells (SnO_2:In_2O_3 /p-Si and SnO_2:In_2O_3/Psi/p-Si) by pulse laser deposition technique annealed and as deposited samples shows that the annealed ones best than as deposited films and the samples deposited on porous Si best than that deposited on Si wafers.

References

[1] K. Zhou, Z. Guo, S. Liu, and J. Lee, "Current Approach in Surface Plasmons for Thin Film and Wire Array Solar Cell Applications," Materials (Basel)., vol. 8, pp. 4565-4581, 2015.

[2] Viswanathan, "study of Cu free back contacts to thin film CdTe solar cell", Ph.D.thesis, university, of south florida, Vol.124, P.(46), (1985).

[3] G. Sivaraman, "Characterization of Cadmium Zinc Telluride Solar Cells," University of South Florida, 2003.

[4] S. C. Ezugwu, "Synthesis and characterization of copper nanoparticles and copper-polymer nanocomposites for plasmonic photovoltaic applications," MSc thesis, The University of Western Ontario, 2012.

[5] D.G. Parker and P. G. Say, "Indium tin oxide/GaAs photodiodes for millimetric-wave applications," *Electronics Letters*, vol. 22, no. 23, pp. 1266-1267, (1986).

[6] W. H. Bragg and W. L. Bragg, X Rays and Crystal Structure. London: G. Bell and Sons, LTD., 1918.

[7] P. Yang, The Chemistry of Nano Structured Materials. Printed in Singapore.: World Scientific Publishing Co. Pte. Ltd., p. 362, 2003.

[8] R.S. Dubey, D. K. Gautam, Optoelectronic Adv. Mater.- Rap. Comm., 9, p.(436), (2007).

[9] J.Zhu, M. Zhou, J. Xu and X. Liao, "preparation of Cds and Zns nanopartical using microwave irradiation" Materials Letter47, p.p(25-29), (2001) .

[10] J.C. Mainfacier, J. Gasiot, and J. P. Fillard, "J. phys. E. Sci. instrum.", 9, (1989).

[11] S. Chan, M. Li, H. Wei, S. Chen, and C. Kuo1, "The Effect of Annealing on Nanothick Indium Tin Oxide Transparent Conductive Films for Touch Sensors" Journal of Nanomaterials, Vol. 2015 (2015).

[12] ZnS Nanocrystals G. Muralia, D. Amaranatha, B. Poornaprakasha, R. Vijayalakshmia,N. Madhusudhana Rao, "Effect Of Annealing On Structural And Optical Properties Of" Optoelectronics And Advanced Materials , vol. 5, no. 9, 2011, p. 928-931.

[13] H. M. Zeyada, M. M. El-Nahass, I. K. El-Zawawi, and E. M. El-Menyawy, "Characterization of 2-(2,3-dihydro-1,5- dimethyl-3-oxo-2-phenyl-1H-pyrazol-4-ylimino)-2-(4-nitrophenyl) acetonitrile and ZnO nano-crystallite structure thin films for application in solar cells," The European Physical Journal, vol. 49, p. 10301, (2010).